



PERGAMON

Applied Radiation and Isotopes 57 (2002) I-XIII

Applied
Radiation and
Isotopes

www.elsevier.com/locate/apradiso

AUTHOR INDEX VOLUME 55

Abbas M. I., 245
Abd El-Maksoud T. M., 135
Abd El-Naby H. H., 861
Abdel-Ghany H. A., 575
Abdel-Haleem A. S., 569, 853, 873
Abdul-Hadi A., 109
Acharya R. N., 595
Adu P. S., 175
Agarande M., 161
Ahmad M., 731
Ahmadian-Pour M. R., 189
Ahmed F., 853, 873
Aitnouh F., 205
Akaho E. H. K., 175, 617
Akram W., 731
Al-Azmi D., 413
Alcaraz Pelegrina J. M., 419
Aldahan A., 715
Alhassanieh O., 109
Ali A. F., 115
Altzitzoglou T., 493
Amer H., 135
Angelone M., 505
Anim-Sampong S., 175, 617
Appoloni C. R., 697
Aragno D., 375
Arif M., 647
Arjun G., 561
Arnold D., 493

Baffa O., 13
Bakaç M., 721
Bandong B. B., 653
Banerjee K., 751
Banjade D. P., 235, 297
Basile S., 259
Bastian Th., 303
Bazioglou M., 339
Bäck T., 157
Bellia S., 259
Benzoubir S., 161
Berrazzouk S., 205
Betenekova T. A., 363
Bianchini G. M., 653
Blackburn B. W., 767
Bodizs D., 103

Bogni A., 17
Bontchev G. D., 293
Borsaru M., 407
Bossus D., 347
Bouisset P., 161
Bozadjiev L. L., 701
Brai M., 259
Bronson F., 493
Bubba T., 505
Buckley K. R., 457
Buraglio N., 715
Byrne A. R., 347

Calmet D., 161
Camargo S. P., 477
Cannizzaro F., 129
Capote Roy R., 493
Cavouras D., 831
Chao J.-H., 549
Chaudhary P. R., 471
Chen F., 13
Chen J., 323
Chen Z.-Q., 793
Cheng J.-P., 793
Cheung T. T. K., 707
Chiadli A., 167
Chichester D. L., 767
Chiozzi P., 737
Christina Melo e Silva M., 899
Chu T.-C., 315, 383, 609, 623, 679, 759
Chun K. S., 457
Chunfu Z., 441
Coenen H. H., 149, 303
Colacicchi S., 71
Covas D. T., 13
Cuéllar S., 849
Czifrus Sz., 103

da Cruz M. T. F., 477
Dagadu C. P. K., 175, 617
Dawood Y. H., 881
Décombaz M., 493
De Corte F., 347, 493
de Hooge M. N., 783
de Sanoit J., 493
De Wispelaere A., 347

Delfin A., 805
Dixon R., 407
Djeffal S., 141
Domnikov V. N., 543
dos Santos J. M. F., 331
Du J., 181

Edelmaier R., 493
El-Bahi S. M., 569, 575, 873
El-Shershaby A., 853
Elejalde C., 521
Elyahyaoui A., 167
Esposito A., 505
Esser B. K., 653
Ewa I. O. B., 103
Ezzahery H., 205

Fattibene P., 375
Füchtner F., 631
Filosofov D. V., 293
Finn R. D., 463
Finn R.D., 667
Fleming D. E. B., 527
Forbes T. A., 527
Frána J., 347
Fujii H., 517
Furetta C., 533

Gano L., 899
García-León M., 849
Garg A. N., 595
Genezini F. A., 477
Ghafar M., 109
Ghahramani A. R., 189
Ghandi M., 789
Ghannadi-Maragheh M., 605
Ghiassi-Nejad M., 189
Giannoni M., 71
Gierga D. P., 767
Günther E., 89
Goncalves I. F., 447
Goto A., 755
Greco G., 129
Gualtieri G., 71
Guzmán-Rincón J., 805
Güven H. H., 9

Hafez A. F., 355
 Hamajima Y., 221
 Hamlat M. S., 141
 Haquin G., 197
 Hassan A. M., 575
 Hassjell S., 433
 Hauser S., 259
 Hemmingsen I. D., 281
 Herranz M., 521
 Herrera Peraza E., 493
 Hiltunen J., 181
 Hirota M., 513
 Hohn A., 149
 Holmberg A. R., 181
 Holschbach M., 309
 Honoki H., 221
 Horák Z., 347
 Hoshi M., 701, 843
 Hsu C.-C., 679
 Hsu H.-H., 323
 Hsu P.-C., 549
 Hurtado E. T., 457
 Hushari M., 115
 Hussain S. D., 731
 Hussein A. S., 355
 Hutchinson E. F., 281
 Hyodo T., 755

Ibrahem N. M., 135
 Ibrahim M. E., 861
 Ido T., 17
 Ignatiev E. A., 363
 Ikeya M., 896
 Inohae E., 899
 Itoh Y., 755
 Ivannikov A. I., 701, 843
 Iwata R., 17

Jafarizadeh M., 189
 Jager P. L., 783
 Jaćimović R., 347
 Jecny Z., 407
 Jensen H. J., 157
 Jin H., 793
 Jivan S., 457
 Jonah S. A., 175, 617
 Juncheng G., 125

Kadi H., 141
 Kalef-Ezra J., 339
 Kandarakis I., 831
 Kanosue K., 896
 Kasch H., 631
 Kateris A., 831
 Kauri T., 427
 Khajmi H., 205

Khalafi H., 605
 Khamidova L. G., 701, 843
 Kheitou M., 115
 Khomichyonok V. V., 701
 Kida T., 229
 Kim J., 755
 Kitis G., 533
 Klein A. T. J., 309
 Klein R., 89
 Klemola S., 493
 Kobashi A., 327
 Kondo T., 221
 Kondrashov A. E., 843
 Kondrashov V. S., 799
 Korun M., 493, 685
 Kralik M., 493
 Kudo A., 427
 Kučera J., 347
 Kumar R., 889
 Kumru M. N., 721
 Kurihara T., 755
 Kyere A. W. K., 175, 617

Lahiri S., 751
 Lapolli A. L., 477
 Lazanin Ž., 267
 Lebedev N. A., 293
 Legarda F., 521
 Lin C.-C., 609
 Lin J.-P., 315, 383, 623, 679, 759
 Lin S.-Y., 315, 383, 679, 759
 Lindegren S., 157
 Liu H.-M., 549
 Liu M.-T., 315, 383, 623
 Lépy M. C., 493
 Luisa Sá e Melo M., 899
 Luurtsema G., 783
 Lyubashevskii N. M., 363

Ma D., 463, 667
 Maakuu B. T., 175, 617
 Manjón G., 849
 Manohar S. B., 751
 Marquez M., 181
 Martinho E., 447
 Martín Sánchez A., 97
 Martínez-Aguirre A., 419
 Mataka S., 899
 Matloubi H., 789
 McDevitt M. R., 463, 667
 Medeiros J. A. G., 477
 Melquiades F. L., 697
 Meriç N., 557
 Minato S., 737
 Miramonti L., 485
 Misdaq M. A., 205

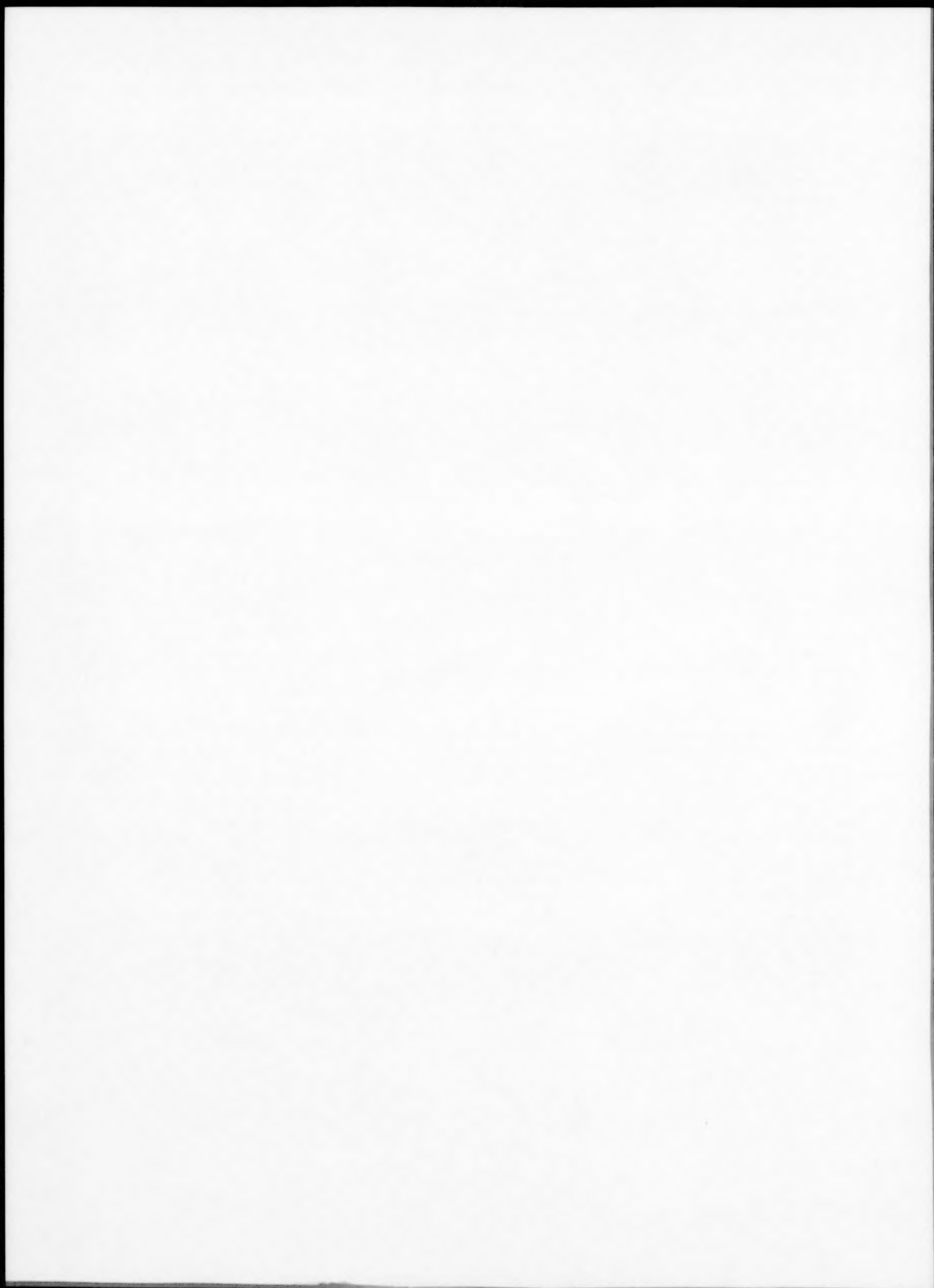
Miyake Y., 17
 Mohapatra D. K., 693
 Molnar Zs., 103
 Monteiro C. M. B., 331
 Mukherjee A., 471
 Mukhopadhyay K., 751
 Murali S., 253
 Murugesan S., 641
 Mushtaq A., 647

Nada A. A., 135
 Nada A., 575
 Nagashima Y., 755
 Nakajima T., 221
 Nakanishi T., 221
 Natarajan V., 253
 Nath R., 813
 Nazari K., 605
 Neder H., 493
 Neronova E., 335
 Nichols A. L., 23
 Nikezić D., 121
 Nikezic D., 707
 Nikiforov A., 335
 Nikiforov S. V., 363
 Nilsson S., 181
 Nir-El Y., 1, 197
 Nishizawa K., 513
 Nomicos C. D., 831
 Norizawa K., 896
 Noronha O. P. D., 641
 Nortier F. M., 149
 Novgorodov A. F., 293

Ogata Y., 513
 Onori S., 375
 O'Meara J. M., 767

Panayiotakis G. S., 831
 Pandey U., 471
 Paredes L. C., 805
 Pascali C., 17
 Pasquale V., 737
 Patil D. D., 289
 Patricio L., 899
 Päch M., 215
 Pervez S., 647
 Piers A., 783
 Pillai M. R. A., 471
 Plagnard J., 493
 Planinić J., 267
 Pohl K. P., 281
 Pommé S., 493
 Possnert G., 715
 Prasad R., 889
 Pushparaja 253

Qaim S. M., 149, 303
 Radolić V., 267
 Rajurkar N. S., 289
 Ramakrishna V. V. S., 595
 Ramamoorthy N., 561
 Ramaswami A., 751
 Raneli M., 129
 Reddy A. V. R., 595
 Reddy C. P., 693
 Ribeiro F. B., 393
 Rivard M. J., 775
 Rizzo S., 259
 Römer J., 631
 Rojc A., 407
 Romero F., 521
 Roque A., 393
 Rosner G., 823
 Rothenberg S. J., 799
 Rubio Montero M. P., 97
 Ruckerbauer F., 273
 Ruth T. J., 457
 Saemian N., 789
 Saito F., 755
 Sajjad M. I., 731
 Saleh G. M., 861
 Salgado J., 447
 Saltykov L. S., 543
 Samuel A. M., 641
 Sanipoli C., 533
 Santopietro F., 533
 Saraswathy P., 561
 Sarkar S. K., 561
 Sasaki T., 427
 Sastry M. D., 253
 Sayed A. M., 413
 Saze T., 513
 Scheinberg D. A., 463
 Scheinberg D. A., 667
 Schönfeld E., 89
 Scholten B., 149
 Schrader H., 89
 Schötzig V., 89
 Sengupta D., 889
 Sgattoni R., 71
 Shamsaii M., 605
 Shawky S., 135
 Shetty S. J., 641
 Shevchenko S. V., 543
 Shishkina E. A., 363
 Shoji M., 221
 Shukri A., 235, 297
 Shweikani R., 115
 Silver G. L., 589
 Sima O., 1, 493
 Simonits A., 347
 Singh A. K., 889
 Skripnik D. D., 701
 Skvortsov V. G., 701, 843
 Slozina N., 335
 Slusarenko L. I., 543
 Smodiš B., 347
 Spitale M. C., 129
 Srivastava T. S., 641
 Sroor A., 569, 873
 Starodub G. Y., 293
 Stehle R., 407
 Steinbach J., 631
 Stepanenko V. F., 701, 843
 Stößer R., 215
 Suzuki K., 229
 Suzuki N., 755
 Tabata T., 125
 Tajuddin A. A., 235, 297
 Takatsuka K., 221
 Takei M., 229
 Takue M., 517
 Takriti S., 115
 Taylor D. M., 285, 745
 Tepehan F. Z., 9
 Tepehan G. G., 9
 Thiemann T., 899
 Tikounov D. D., 843
 Tikunov D. D., 701
 Tolstykh E. I., 363
 Tomarchio E., 129
 Tsoukos S., 831
 Ugletveit F., 493
 Ureña-Nuñez F., 805
 Urošević V., 121
 Uğur (Tanbay) A., 581
 Vaca F., 849
 van der Walt T. N., 149
 van Sluijs R., 347
 Van Velzen L., 493
 Vasilik D. G., 323
 Venkataramani R., 253
 Venkatesh M., 471
 Verdoya M., 737
 Vidmar T., 493
 Vojtyla P., 81
 Volpe A. M., 653
 Wallace G., 281
 Walley El-Dine N., 853
 Wang X., 453
 Wei L., 755
 Winkler R., 273, 823
 Wu G., 895
 Xiuli Z., 441
 Yanai K., 17
 Yanch J. C., 767
 Yanli Z., 125
 Yatim H. A., 413
 Yener G., 581
 Yongping Z., 441
 Yongxian W., 441
 Yu K. N., 707
 Yuandi Y., 125
 Yuda Z., 125
 Yue N., 813
 Zafar M. S., 731
 Zamboni C. B., 477
 Zambrano F., 805
 Zarki R., 167
 Zarrindast M.-R., 789
 Özben C. S., 9
 Zeisler S., 457
 Zevallos-Chávez J. Y., 477
 Zhang J., 453
 Zhang L., 793
 Zohny E., 569





PERGAMON

Applied Radiation and Isotopes 57 (2002) XV-XXVIII

Applied
Radiation and
Isotopes

www.elsevier.com/locate/apradiso

SUBJECT INDEX VOLUME 55

Accelerator

Based: feasibility of NAA of nitrogen	767
CERN: calibration of monitors for radioactivity in effluent water	81
Linear, photon and electron beams: comparison of various protocols for determination of absorbed dose	235
PRIMUS: Monte Carlo simulation of dose distribution in water	759
Siemens Primus linear: measurement of photo neutrons in the vicinity	315*

Actinium

^{225}Ac breakthrough together with daughters from a $^{225}\text{Ac}/^{213}\text{Bi}$ generator: study	667
--	-----

Activation analysis

NAA	
Elemental investigation of Egyptian motor vehicle alloys	575
Kay zero assisted: installation and calibration in central Europe	347
Of nitrogen: feasibility of use of an accelerator	767
Use for thin film thickness determination	9
Use of gold as a monostandard	595
Use to determine heavy metals and rare earth elements in phosphate fertilizer	569

Adsorption

Of ^{131}I on platinum-charcoal for separation from irradiated uranium	605
---	-----

Alanine

Dosimeter: evaluation for determination of irradiation dose to blood	13
--	----

Albedo

Measurement to assay nuclear materials in solutions	693
---	-----

Alloy

Egyptian motor vehicle: elemental analysis by NAA	575
---	-----

Alpha particle

Activity monitoring of airborne particles: effectiveness of spectrometry	543
Emitting radio-immunopharmaceuticals: preparation	463
Evaluation of activity of radon and thoron in natural samples by SSNTD	205
Source: U(VI) and Th(IV) by electrodeposition in presence of Cu^{2+} and trivalent metals	167

Alumina

Chromatographic column: use to extend the life of a $^{99\text{m}}\text{Tc}$ generator	561
--	-----

Americium

^{241}Am in sediments: determination by isotope dilution high resolution inductively coupled plasma mass spectrometry	161
--	-----

Analyser

Nucleonic: for determination of coal ash of the coal face or the surface of stockpiles	407
--	-----

* Indicates a Technical Note.

† Indicates a Letter to the Editor.

Antibody

Monoclonal: HuM195-CHX-A-DTPA conjugation with ^{213}Bi for use in radio-immunotherapy 463

Arrhenius curve

Models for a peak: comments on radiation effects in dry ice 895[†], 896[†]

Ash

Coal: portable nucleonic analyser for determination at the coal face or on stockpiles 407

Volcanic: use of thin layer activation for on-line erosion monitoring 281

Astatine

^{211}At : dry distillation from irradiated Bi targets 157

Atmosphere

Of Kuwait 1994-8: variations in ^7Be concentrations 413

Background

Signal in tooth enamel: elimination for EPR dosimetry 701

Bacteria

Anaerobic: effect of pH and temperature on sorption of Np and Pa 427

Barium

^{139}Ba decay: α -ray spectra of ^{139}La product 477

Beam

Electron, dose: comparison of discrepancy between chemical dosimeters and calorimeter 125

Electron and photon: determination of absorbed dose from a linear accelerator by comparing various protocols on different phantoms 235

Electron and photon: use of *Rhizophora* spp. wood phantom for dosimetric purposes 297

Beryllium

^7Be concentrations in atmosphere of Kuwait 1994-8 413

^7Be : local and collector surface effects in sampling for determination of deposition to ground 823

Bismuth

^{213}Bi : generator produced for conjugation with monoclonal antibodies 463

^{213}Bi production from ^{225}Ac : development of generator and evaluation 667

Irradiated target: separation of ^{211}At by dry distillation 157

Blood

Dicentrics persistence in Chernobyl clean-up workers 335

Irradiation: determination of dose using an alanine/ESR dosimeter 13

Body

Total irradiation therapy: dose compensation 623

Bone

Digital XRF system for lead: calibration and characterisation 527

In vivo lead analysis: calculation of Pb concentration and uncertainty in XRF 799

Book

Pages printed in the 1960s in Japan: ^{137}Cs content 327

Review of radioactivity in the environment 745

Boron

^{10}B estimation in heavy water by neutron reflection method 693

LS-1-BrachyseedTM

Interstitial brachytherapy ^{125}I source: dosimetric characterization 813

Brachytherapy

Dosimetric characteristics of ^{192}Ir sources 189

Interstitial source of ^{125}I (model LS-1-BrachyseedTM) 813

TG-43 dosimetry parameters: discretized approach using Monte Carlo calculations for the

MED 3633 ^{103}Pd source 775

Brain	
Imaging: preparation of $^{99m}\text{TcN}(\text{CBDTC})_2$ and biodistribution in mice	453
Building	
Materials: α -activity in Sicily	259
Calcium	
$\text{CaSO}_4\text{:Dy}$: evaluation for ESR dosimetry	253
Calorimeter	
Dose measurement for an electron beam: discrepancy with a chemical dosimeter	125
Carbon dioxide	
Dry ice: comments on radiation effects and models for a peak on the Arrhenius curve	895 [†] , 896 [†]
Cement	
Radon diffusion through varying depths	115
Cesium	
Bromide: electrolytic diffusion coefficient in water	289
^{137}Cs contained in books printed during 1960s in Japan	327
^{137}Cs : local and collector surface effects in sampling for determination of deposition to ground	823
Charcoal	
Activated: in radon measurement and simulation of skim-off method	121
Platinum sorbent: use to separate ^{131}I from natural uranium fission products	605
Chernobyl	
Accident: EPR dosimetry of dental enamel of children	71
Clean-up workers: persistence of dicentrics after low doses of radiation	335
Children	
Dental enamel: EPR dosimetry after Chernobyl accident	71
Chromatography	
Alumina column: feasibility of extending life of a ^{99m}Tc generator	561
Ion exchange: use in concentration and purification of ^{111}In radiochemicals	293
$11-[^{14}\text{C}]\text{-Clozapine}$ {8-chloro-11-(4-methyl-1-piperazinyl)-11-[^{14}C]-5H dibenzo[b,e][1,4]diazapine}	
Synthesis	789
Coal	
Portable analyser for determining ash on the coal face and on stockpiles	407
Code	
CYLTRAN: use for radiation transport and dose calculations for material interfaces	323
GEANT3.21: use for simulation to determine monitor efficiency for radioactivity in effluent water	81
MCNP: use to calculate epithermal neutron resonance self shielding factors in wires	447
OMEGA/BEAM: use in Monte Carlo simulation of dose distribution due to a clinical linear accelerator	759
Container	
Large, inspection system: geometrical rectification of images	793
Copernicus project	
Installation and calibration of Kay-zero-assisted NNA in 3 central European countries	347
Copper	
U mineralization: radiometric prospecting on rocks in Singhbhum area of Bihar	889*
Counter	
Gas flow proportional: use for determination of ^{90}Sr and factor of merit and minimum detectable activity	849*
Counting	
Foggy scintillator technique	517

Gas flow proportional or Cherenkov: factor of merit and minimum detectable activity for ^{90}Sr <i>CR-39</i>	849*
Monte Carlo calculation for determining detection efficiency for α -particles from radon and thoron <i>Cyclam acid porphyrin (CAP)</i>	205
$^{99\text{m}}\text{Tc}$ labelled: use in tumour imaging	641
<i>Cyclotron</i>	
Production of n.c.a. ^{103}Pd	441
<i>Dating</i>	
Disequilibrium: of secondary uranium ore from the south Eastern Desert of Egypt	881
<i>Decay</i>	
Data of ^{177}Lu and ^{188}Re and standardisation	89
Data: review of measurements, evaluations and compilations	23
Of ^{139}Ba and energy levels of ^{139}La decay product	477
<i>Deposition</i>	
Atmospheric, of $^{239} + ^{240}\text{Pu}$ and ^{238}Pu in an arid area of Spain: activity	97
^{137}Cs and ^7Be on ground: dependence on local and collector surface effects in sampling	823
<i>Depth</i>	
Dose measurements using a <i>Rhizophora</i> spp. wood phantom for electron and photon beams	297
<i>Detective quantum efficiency</i>	
Theoretical model for calculation in granular scintillators	831
<i>Detector</i>	
BD-PNP bubble: use in measurement of photoneutrons in the vicinity of a Siemens Primus linear accelerator	315*
Calibration for radioactivity in effluent water from CERN accelerator	81
<i>HPGe</i>	
Angular response to γ -rays in in situ measurements	1
Monte Carlo determination of full energy peak efficiency	103
Response to X-rays with energy in the region of Ge k-absorption edge	331
Polymeric track: use to determine Rn concentrations in Egyptian tombs	355
Positron: development for PET metabolites	229
Scintillation: low energy threshold for X- and γ -rays at Fréjus underground laboratory	485
Solid state nuclear track: efficiency for Rn and Th in natural samples	205
Ultra thin TL: use for skin dose measurements	383
Well type NaI(Tl) and HPGe: analytical formulae for efficiency computation	245
X-ray, mobile system for large containers: rectification of images	793
<i>Dicentrics</i>	
Persistence in blood of low dose Chernobyl clean-up workers	335
<i>Diffusion</i>	
Electrolytic coefficient of CsBr in water	289
<i>Dimethyl sulfoxide</i>	
Competing labelling during ^{11}C methylation of amine precursors	309
<i>Distillation</i>	
Dry: use to separate ^{211}At from irradiated Bi targets	157
<i>sym-Di[4(5)tert-butylbenzo]-16-crown-5-oxyacetic acid (DTBDB16C5-OAcH)</i>	
Use in solvent extraction of radium	609
<i>Dose</i>	
Absorbed due to ^{90}Sr in dental tissue: comparison of Monte Carlo calculation to EPR measurement	363
Absorbed from photon and electron beams: comparison of determination by different protocols on different phantoms	235
Absorbed in <i>Drosophila melanogaster</i> when neutron irradiated	805

Air absorbed rate due to natural radiation in the Aeolian volcanic arc	737
Compensation of total body irradiation therapy	623
Depth distribution in calorimeter and dosimeter for an electron beam: discrepancy in measurements	125
Determination for the lens of the eye by Monte Carlo calculation	557
Distribution in water: Monte Carlo simulation for PRIMUS clinical linear accelerator	759
Due to radon activity in ancient Egyptian tombs	355
Enhancement from photon beams at material interfaces	323
Gamma rate from building materials used in Sicily	259
High rate measurement by photon activation of indium foils	549
Measurement for skin using ultra thin TLDs	383
Reconstruction by EPR spectroscopy: use of porcelain insulators	843
<i>Dosimeter</i>	
Alanine: evaluation for determination of radiation dose to blood	13
Bronchial: design for measurement of radon progeny	707
Chemical: discrepancy with calorimeter dose measurement for an electron beam	125
Thermoluminescent: response to low energy protons in the range 30–100 keV	697
<i>Dosimetry</i>	
Characterization of an encapsulated interstitial brachytherapy source of ^{125}I : model—LS1-Brachyseed TM	813
EPR: elimination of background signal in tooth enamel samples	701
EPR: on dental enamel of children after Chernobyl accident	71
ESR: study of Li_2CO_3 and $\text{CaSO}_4:\text{Dy}$ as prospective dosimeters	253
TG-43 brachytherapy parameters: Monte Carlo calculations for the MED 3633 ^{103}Pd source	775
TL: study of thermoluminescent properties of perovskite (KMgF_3) activated by Ce and Er impurities	533
Use of <i>Rhizophora</i> spp. wood phantom in measurements on electron and photon beams	297
With radiochromic films: evaluation	339
<i>Drosophila melanogaster</i>	
Determination of absorbed dose from neutron irradiation and genetic effects	805
<i>Earthquake</i>	
Effect on radon levels in soil	267
<i>Electrodeposition</i>	
Method of preparation of U(VI) and Th(IV) α -sources in presence of Ca^{2+} and trivalent metals	167
<i>Element</i>	
Concentration in environmental SRMs and river sediments by k_o method using gold as a monostandard	595
<i>Enamel</i>	
Dental: EPR dosimetry after Chernobyl accident	71
Tooth: elimination of background signal in EPR dosimetry	701
Tooth: mechanically induced EPR signals during sample preparation	375
<i>EPR</i>	
Dosimetry on dental enamel of children after Chernobyl accident	71
Measurement of ^{90}Sr absorbed dose in dental tissue: comparison with Monte Carlo calculations	363
Signal: mechanical induction in tooth enamel	375
Spectroscopy: use of porcelain insulators for dose reconstruction	843
<i>Erosion</i>	
Monitoring: use in thin layer activation	281

Erratum

Correction to author's address in 'Synthesis and biological evaluation of two radiolabelled estrogens' (JARI 54, p. 227) 899

ESR

Dosimetry: evaluation of Li_2Co_3 and $\text{CaSO}_4\text{:Dy}$ as prospective dosimeters 253
 Spectroscopy for H-atoms and free radicals trapped in octasilsesquioxanes 215

Estrogen

Correction to address of M. Cristina Melo e Silva in JARI 54 227 899

EUROMET project

For intercomparison of efficiency transfer software for γ -ray spectrometry 493

Excitation functions

Of $^{124}\text{Te}(\text{d},\text{xn})^{124,125}\text{I}$ reactions with reference to production of ^{124}I 303
 Of $^{125}\text{Te}(\text{p},\text{xn})$ reactions with reference to production of ^{124}I 149

Fertilizer

Factory in S. Spain: effect on natural radioactivity in surrounding groundwater 419
 Phosphate: determination of heavy metals and rare earth elements by NAA 569

Film

Raadiochromic: dose assessment by document scanner technique, neutron response and applications 339

Thickness: determination by NAA 9

Fluoride

^{18}F -fluoride: production in high yield from gas target 457

Fluorine

^{18}F labelled: electrochemical production from $[^{18}\text{O}]$ water 755

16 α -[^{18}F]-Fluoroestradiol-3,17 β -disulphamate

Synthesis 631

Formula

For efficiency computation for well type $\text{NaI}(\text{Tl})$ and HPGe detectors 245

Free radical

Trapping with octasilsesquioxanes for ESR spectroscopy 215

Gamma ray

Activity and dose rate from building materials in Sicily 259

Angular response of a HPGe detector in in situ measurements 1

Emission probabilities of ^{177}Lu and ^{188}Re 89

Low energy threshold detector at Fréjus underground laboratory 485

Natural radiation in the volcanic Aeolian arc 737

Gas

Industry: assessment of radiation exposure to NOR materials 141*

Generator

$^{225}\text{Ac}/^{213}\text{Bi}$: development and quantitative studies 667

^{212}Pb based on a ^{228}Th source 33

^{99}Tc : extension of life by using an alumina chromatographic column 561

Germanium

Detector: response to X-rays with energy in region of the Ge k-absorption edge 331

Glycosylated somatostatin-14

$^{99\text{m}}\text{Tc}$ labelling 181

Gold

Use as a monostandard for determination of elemental concentrations in SRMs and Ganga river sediments 595

<i>Granite</i>	
Measurement of radioactivity and radon exhalation rate	853
Two mica, of Gabal Ribdah, Egypt: uranium and thorium mineralization	861
<i>Half life</i>	
Of ^{177}Lu and ^{188}Re	89
<i>Heat</i>	
Volumetric production rates in sediments of the São Francisco basin, Brazil	393
<i>HPLC</i>	
Use in the measurement of positron emitters	229
<i>Hydrogen</i>	
Atoms: use of octasilsesquioxanes as trapping agents for ESR spectroscopy	215
Total, in Ghanian petroleum products: measurement by thermal neutron reflection method	617
<i>Hydroxy apatite</i>	
^{90}Y labelled particles: preparation for synovectomy	471
<i>Imaging</i>	
Of large containers: geometrical rectification of images from a mobile system	793
Plate: use in feasibility study of in vivo thyroid ^{131}I monitoring	513
<i>Indium</i>	
Foils: measurement of high dose rates by photon activation	549
^{111}In radiochemicals: production, concentration and purification	293
<i>Interface</i>	
Material: photon radiation dose enhancement	323
<i>Iodine</i>	
^{124}I thick target yield: excitation functions of $^{125}\text{Te}(\text{p},\text{xn})$ reactions	149
^{124}I thick target yield: excitation functions of $^{124}\text{Te}(\text{d},\text{xn})^{124,125}\text{I}$ reactions	303
^{125}I brachytherapy source (model LS 1-Brachyseed TM): dosimetric characterization	813
^{129}I in lakes in Chernobyl fallout region	715
^{131}I in vivo monitoring in the thyroid: feasibility	513
^{131}I separation from natural uranium fission products	605
<i>L-3-[^{123}I]Iodoalpha-methyl tyrosine</i>	
Synthesis	783
<i>Iridium</i>	
^{192}Ir sources: dosimetric characteristics when used in interstitial brachytherapy	189
<i>Iron</i>	
^{90}Y labelled ferric hydroxide macroaggregates: preparation for radiation synovectomy	47
<i>k_o method</i>	
For elemental concentrations in the environmental SRMs and sediments	595
<i>Lanreotide</i>	
Direct labelling with $^{99\text{m}}\text{Tc}$	647
<i>Lanthanum</i>	
^{139}La energy levels following decay of ^{139}Ba	477
<i>Lead</i>	
Concentration and its uncertainty in XRF in vivo analysis in bone	799
In bone: digital XRF system calibration and characterisation	527
^{210}Pb dating in sediments in Gökova Bay (Aegean sea—Turkish coast)	581
^{210}Pb in air filters: evaluation of a low level spectrometer with a planar low energy HPGe shield	129*
^{212}Pb generator based on a ^{228}Th source	433

<i>Lens</i>	
Eye: calculation of radiation dose using Monte Carlo simulation	557
<i>Lithium</i>	
Li ₂ CO ₃ : evaluation for ESR dosimetry	253
<i>LR-115 II</i>	
Monte Carlo calculation for determining detection efficiency for α -particles from radon and thoron	205
<i>Lutetium</i>	
¹⁷⁷ Lu standardisation and decay data	89
<i>Marble</i>	
Measurement of radioactivity and radon exhalation rate	853
<i>Marinelli beaker</i>	
Use in γ -ray spectrometry of powdered milk samples	697
<i>Mass attenuation coefficients</i>	
Measurement for elemental materials in range $6 \leq Z \leq 82$ using X-rays from 13–50 keV	505
Uncertainties: effect on counting efficiency in γ -spectrometry	685
<i>Material</i>	
Elemental in range $6 \leq Z \leq 82$: measurement of mass attenuation coefficients	505
<i>Metal</i>	
Heavy, in phosphate fertilizers: determination by NAA	569
<i>Milk</i>	
Powder: self absorption correction for γ -spectrometry using Marinelli beakers	697
<i>Monte Carlo</i>	
Calculation of epithermal neutron resonance self shielding factors in wires	447
Calculation of ⁹⁰ Sr absorbed dose in dental tissues: comparison with EPR measurements	363
Calculations for the MED 3633 ¹⁰³ Pd source using a discretized approach	775
Computer code for determining detection efficiency of CR-39 and LR115II solid state track detectors	205
Determination of full energy peak efficiency for HPGe detector	103
<i>Simulation</i>	
For intercomparison of efficiency transfer software for γ -ray spectrometry	493
For radioactivity measurements in effluent water from CERN accelerator	81
Of a clinical linear accelerator	759
Of albedo of thermal neutrons and use for assay of nuclear materials in solutions	693
Of angular response of a HPGe detector to γ -rays in in situ measurements	1
Use in calculation of radiation dose to the lens of the eye	557
<i>Methyl iodide</i>	
[¹¹ C] labelled: use in ¹¹ C methylation of amine precursors and competition of solvent DMSO	309
<i>[¹¹C] Methyl triflate</i>	
Use in preparation of [¹¹ C] raclopride by a simple loop method	17
<i>Neptunium</i>	
Effect of pH and temperature on sorption to mixed anaerobic bacteria	427
<i>Neutron</i>	
Epithermal, resonance self shielding factors in wires: Monte Carlo calculations	447
Irradiation of <i>Drosophila melenogaster</i> : determination of absorbed dose and induced genetic effects	805
Photo: measurement in vicinity of a Siemens Primus accelerator	315*
Response of radiochromic films	339
<i>Thermal</i>	
Reflection: geometrical effects of hydrogenous moderators using a ²⁴¹ Am–Be source	175

Reflection method for measurement of total hydrogen in petroleum products	617
Reflection method to assay nuclear materials in solutions	693
<i>Nitrogen</i>	
In vivo NAA: feasibility of using an accelerator	767
<i>Octasilsesquioxane</i>	
Use as a trapping cage for H-atoms and free radicals	215
<i>Oil</i>	
Industry: assessment of radiation exposure to NOR materials	141*
Industry in E and W deserts of Egypt: characteristics of NOR	135
Products, Ghanian: total hydrogen content by thermal reflection method	617
<i>Oxygen</i>	
$^{18}\text{O}(\text{p},\text{n})^{18}\text{F}$ reaction: application to targetry	457
^{16}O beam: use to irradiate a thulium target with production of ^{181}Re	751
<i>Palladium</i>	
^{103}Pd n.c.a. : cyclotron production by bombardment of a rhodium target	441
^{103}Pd source: Monte Carlo calculations to determine the TG-43 brachytherapy dosimetry parameters	775
<i>Paraffin</i>	
Moderator: geometrical effects on thermal neutron reflections using a $^{241}\text{Am}-\text{Be}$ source	175
<i>Particle</i>	
Airborne: effectiveness of spectrometry in α -activity monitoring	543
<i>Peak</i>	
Full energy efficiency: Monte Carlo determination for a HPGe detector	103
<i>Perovskite (KMgF₃)</i>	
Activated by Ce and Er impurities: thermoluminescent properties	533
<i>PET</i>	
Metabolites: measurement after elution by HPLC	229
Synthesis of $16\alpha-[^{18}\text{F}]$ fluoroestradiol-3,17 β -disulphamate for use as a tracer	631
<i>pH</i>	
Effect on sorption of Np and Pa to mixed anaerobic bacteria	427
<i>Phantom</i>	
PMMA: use in determination of dosimetric characteristics of ^{192}Ir brachytherapy sources	189
Rando: use in dose compensation studies of total body irradiation	623
<i>Rhizophora</i> spp. wood: use for dosimetric purposes for high energy photon and electron beams	297
Use in determination of absorbed dose for photon and electron beams comparing different protocols	235
<i>Phosphor</i>	
Li_2CO_3 and CaSO_4 : DY: evaluation for ESR dosimetry	253
<i>Photon</i>	
Activation of indium foils: application to measurement of high dose rates	549
Radiation dose enhancement at material interfaces	323
<i>Platinum</i>	
Charcoal sorbent to separate ^{131}I from irradiated uranium	605
<i>Plutonium</i>	
Oxidation states in sea water	589
$^{239+240}\text{Pu}$ and ^{238}Pu activity in atmospheric deposits	97
<i>Polyethylene</i>	
Layer: prevention of radon diffusion into cement	115
<i>Porcelain</i>	
Insulators: possible use for radiation dose reconstruction by EPR spectroscopy	843

<i>Positron</i>	
Emitters: development of detector	229
<i>Potassium</i>	
^{40}K : γ -dose rate from building materials in Sicily	259
KMgF_3 activated by Ce and Er impurities: thermoluminescent properties	533
Vertical distribution in sediments of São Francisco Basin, Brazil	393
<i>Protactinium</i>	
Effect of pH and temperature on sorption to mixed anaerobic bacteria	427
<i>Protocol</i>	
AAPM,HPA,IAEA,IPEMP: comparison for absorbed dose determination	235
<i>Proton</i>	
30–100 keV: response of a thermoluminescent dosimeter	679
<i>[^{11}C]Raclopride</i>	
Automated preparation by a simple loop method from [^{11}C] methyl triflate	17
<i>Radiation</i>	
Low dose to Chernobyl clean-up workers: persistence of dicentrics in blood	335
Total body therapy: dose compensation	623
<i>Radioactivity</i>	
Deposition to ground of nuclides: dependency on local and collector surface effects in sampling	823
Measurement in different types of marble and granite	853
Measurement in effluent water from CERN accelerator: calibration of monitors	81
Minimum level detectable in in situ γ -spectrometry	197
Natural: effect of waste from fertilizer plant in S. Spain	419
Natural, in soil in southern Egypt	873
<i>Radioimmunotherapy</i>	
Preparation of ^{213}Bi for α -particle therapy	463
<i>Radiometric prospecting</i>	
On rocks with Cu–U mineralization in the Singhbhum zone of Bihar	889*
<i>Radionuclide</i>	
Naturally occurring	
Assessment of exposures to personnel in the oil and gas industry	141*
Characteristics in oil extracted from E and W deserts of Egypt	135
Preconcentration and measurement of low levels of γ -emitters in coastal waters	653
<i>Radiopharmaceutical</i>	
Preparation of $^{99\text{m}}\text{TcN}(\text{CBDTC})_2$	453
Short lived α -emitting: preparation for radioimmunotherapy	463
<i>Radium</i>	
Gamma dose rate from building materials in Sicily	259
Solvent extraction using sym-di[4(5)-tert-butylbenzo]-16-crown-5-oxyacetic acid	609
<i>Radon</i>	
Bronchial dosimeter design for measurement of progeny	707
Concentration and effective doses in ancient Egyptian tombs	355
Concentration in soil gas: comparison of methods of determination	273
Diffusion through varying depths of cement	115
Evaluation of α -activity per unit volume of natural samples using SSNTD	205
Exhalation rate	
In rocks with Cu–U mineralization in Singhbhum zone, Bihar	889*
In soil in southern Egypt	873
Measurement in different types of marble and granite	853

Indoor levels from building materials in Sicily	259
Measurement by activated charcoal: simulation of skim-off method	121
Temporal variations in soil related to earthquakes	267
<i>Rare earth element</i>	
Determination in phosphate fertilizer by NAA	569
<i>Resonance self shielding factor</i>	
Monte Carlo calculation for epithermal; neutrons in wires	447
<i>Rhenium</i>	
^{181}Re : separation carrier free from ^{16}O -irradiated thulium target	751
^{188}Re : standardization of decay data	89
<i>Rhodium</i>	
Target: use in cyclotron production of ^{103}Pd	441
<i>Rice</i>	
Straw paper: ^{137}Cs content in the 1960s in Japan	327
<i>Rock</i>	
Aeolian volcanic arc: natural γ -radiation	737
Sedimentary in São Francisco basin, Brazil: vertical distribution on U, Th and K and volumetric heat production	393
<i>Sample</i>	
Cu-U mineralised in the Singhbhum zone, Bihar: radon exhalation and radiometric prospecting	889*
Environmental: minimum detectable activity by in situ γ -spectrometry	197
Natural: radon and thoron detection by SSNTD	205
Powdered milk: self absorption correction for γ -ray spectrometry measurements	697
Uncertainties in counting efficiency in γ -ray spectrometry	685
<i>Scanner</i>	
Document: use for reading radiochromic films for dose assessment	339
<i>Scintillator</i>	
Granular: calculation of the detective quantum efficiency (DQE)	831
<i>Sediment</i>	
^{241}Am determination by ID-HR-ICP-MS	161
Deposition and accumulation rate in the Gökova Bay (Aegean Sea-Turkish coast)	581
In West Turkey: factor analysis applied to distribution of elements	721
Of São Francisco Basin, Brazil: vertical distribution of U,Th and K and volumetric heat production rates	393
River: use of gold as a monostandard in NAA by k_o method	595
<i>Skin</i>	
Dose measurement using ultra thin TLDs	383
<i>Software</i>	
Efficiency transfer for γ -ray spectrometry: intercomparison	493
Kay zero/Solcoi: use with Kay zero-assisted NAA facilities	347
<i>Soil</i>	
Gas: radon concentration determination and comparison of methods	273
Southern Egypt: natural radioactivity and radon exhalation rate	873
^{90}Sr content from Biscay, Spain	521
Temporal variations of radon related to earthquakes	267
West Turkey: factor analysis applied to distribution of elements	721
<i>Solid state nuclear track detector (SSNTD)</i>	
Efficiency for radon and thoron in natural samples	205

<i>Solvent</i>	
DMSO: labelling side reaction of methylations with n.c.a. [¹¹ C]CH ₃ I	309
[DTBDB]16C5-OAcH: use for extraction of radium	609
<i>Somatostatin</i>	
Analog-Lanreotide: direct labelling with ^{99m} Tc	647
<i>Spectrometer</i>	
ESR: use in evaluation of alanine dosimeters for blood irradiation measurements	13
Ge-X-ray: EUROMET intercomparison of efficiency transfer software	493
Liquid scintillation: use for ⁹⁰ Sr determinations and factor of merit and minimum detectable activity	849*
Low level, using planar HPGe shielding: tests and system performance for ²¹⁰ Pb determination in air filter samples	129*
<i>Spectrometry</i>	
α -: effectiveness in monitoring α -activity in industrial airborne particles	543
α -: use to determine activity of ²³⁹⁺²⁴⁰ Pu and ²³⁸ Pu in atmospheric deposits in Spain	97
γ -ray	
In situ: minimum detectable activity	197
Intercomparison of efficiency transfer software	493
Self absorption correction for powdered milk samples	697
Uncertainties in sample properties and counting efficiency	685
Use to discriminate between natural and depleted uranium	221
Isotope dilution, high resolution, inductively coupled plasma, mass (ID HR ICP MS): use for determination of ²⁴¹ Am in sediments	161
<i>Spectroscopy</i>	
Digital XRF bone lead system: calibration and characterisation	527
EPR: dose reconstruction from irradiated porcelain insulators	843
ESR of H-atoms trapped in octasilsesquioxanes	215
<i>SRM,s (standard reference materials)</i>	
Element concentrations by k_o -method and use of gold as a monostandard	595
<i>Strontium</i>	
⁹⁰ Sr	
Content in soils from Biscay, Spain	521
Determinations: factor of merit and minimum detectable activity by gas flow proportional and Cherekov counting	849*
In dental tissue: comparison of dose calculation to EPR measurement	363
<i>Synovectomy</i>	
Preparation and studies of ⁹⁰ Y labelled particles	471
<i>Target</i>	
Gas: proof of principle for production of ¹⁸ F fluoride	457
Rhodium: use for ¹⁰³ Pd production	441
Silver, irradiated: separation on ¹¹¹ In	293
Thulium, ¹⁶ O irradiated: for production of ¹⁸¹ Re	751
<i>Technetium</i>	
^{99m} Tc generator: extension of useful life by using an alumina chromatographic column	561
^{99m} Tc labelling of glycosylated-somatostatin-14	181
^{99m} TcN(CDTC)2: preparation and biodistribution in mice	453
^{99m} Tc: use to label Lanreotide	647
<i>Teeth</i>	
EPR dosimetry on dental enamel of children after the Chernobyl accident	71
⁹⁰ Sr absorbed dose calculation by Monte Carlo simulation: comparison to EPR measurements	363

Tellurium	
$^{124}\text{Te}(\text{d},\text{xn})^{124,125}\text{I}$ reactions: excitation functions with reference to ^{124}I production	303
$^{125}\text{Te}(\text{p},\text{xn})$ reactions: excitation functions with reference to production of ^{124}I	149
Temperature	
Effect on sorption of Np and Pa to mixed anaerobic bacteria	427
Thermoluminescent compound	
Evaluation of Li_2CO_3 and $\text{CaSO}_4:\text{Dy}$ for ESR dosimetry	253
KMgF_3 (perovskite) activated by Ce and Er impurities; properties	533
Thickness	
Determination of thin films by NAA	9
Thin layer activation technique	
Application for on-line erosion monitoring	281
Thorium	
Distribution in soil and sediment in W. Turkey: factor analysis	721
Mineralization in two mica granite of Gabal Ribdah area, Egypt	861
$^{[228]\text{Th}}$ barium sulfate source: use for a ^{212}Pb generator	433
Th(IV) source : preparation by electrodeposition in presence of Ca^{2+} and trivalent metals	167
Vertical distribution in sediments of São Francisco basin, Brazil	393
Thoron	
Evaluation of α -activity per unit volume of natural samples using SSNTD	205
Thulium	
^{16}O irradiated target: use to produce carrier free ^{181}Re	751
Thyroid	
Feasibility of in vivo ^{131}I monitoring with an imaging plate	513
Tissue	
Dental: ^{90}Sr absorbed dose calculation and comparison to EPR measurements	363
Tomb	
Ancient Egyptian: radon activity concentrations and effective doses	355
Tumour	
Imaging: use of $^{99\text{m}}\text{Tc}$ labelled cyclam acid porphyrin(CAP)	641
Uranium	
Content in rock in the Aeolian volcanic arc and air absorbed dose rate	737
Cu mineralization of rocks in Singhbhum zone, Bihar: radiometric prospecting	889*
Distribution in soil and sediments in W. Turkey: factor analysis	721
Isotopes: disequilibrium in some Syrian groundwater	109
Mineralization in two mica granite of Gabal Ribdah area, Egypt	861
Natural and depleted: discrimination by γ -spectrometry	221
Ore from south eastern desert of Egypt: series disequilibrium dating	881
U(VI) source preparation by electrodeposition in presence of Ca^{2+} and trivalent metals	167
Vertical distribution in sediments of São Francisco basin, Brazil	393
Water	
Coastal: preconcentration and measurement of low levels of γ -emitting radioisotopes	653
Effluent from CERN accelerator: calibration of monitors for radioactivity measurements	81
Electrolytic diffusion coefficient of CsBr	289
Geothermal in Murtazabad area, Pakistan: origin and subsurface history	731
Ground: effect of fertilizer plant in S. Spain and natural radioactivity	419
Ground, in Syria: disequilibrium of uranium isotopes	109
Lake: ^{129}I concentrations resulting from Chernobyl and environmental implications	715
Moderator: geometrical effect on thermal neutron reflection using a $^{241}\text{Am-Be}$ source	175

¹⁸ O labelled: use in the electrochemical production of ¹⁸ F	755
Rain: activity of ²³⁹⁺²⁴⁰ Pu and ²³⁸ Pu from the atmosphere	97
Sea: plutonium oxidation states	589
<i>Wire</i>	
Monte Carlo calculation of epithermal neutron resonance self shielding factors	447
<i>Wood</i>	
<i>Rhizophora</i> spp.: study for use as a phantom for photon and electron beam dosimetry	297
<i>X-ray</i>	
Emission probabilities for decay of ¹⁷⁷ Lu and ¹⁸⁸ Re	89
Fluorescence bone-lead system: calibration and characterisation	527
Low energy threshold scintillation detector at Fréjus underground laboratory	485
Use in measurement of mass attenuation coefficients of elemental materials in range $6 \leq Z \leq 82$	505
With energy in Ge <i>k</i> -absorption edge: effect on response of HPGe detectors	331
XRF: lead concentration and uncertainty in <i>in vivo</i> analysis in bone	799
<i>Yttrium</i>	
⁹⁰ Y labelled particles for use in radiation synovectomy: preparation and studies	471

